CZECH TECHNICAL UNIVERSITY IN PRAGUE

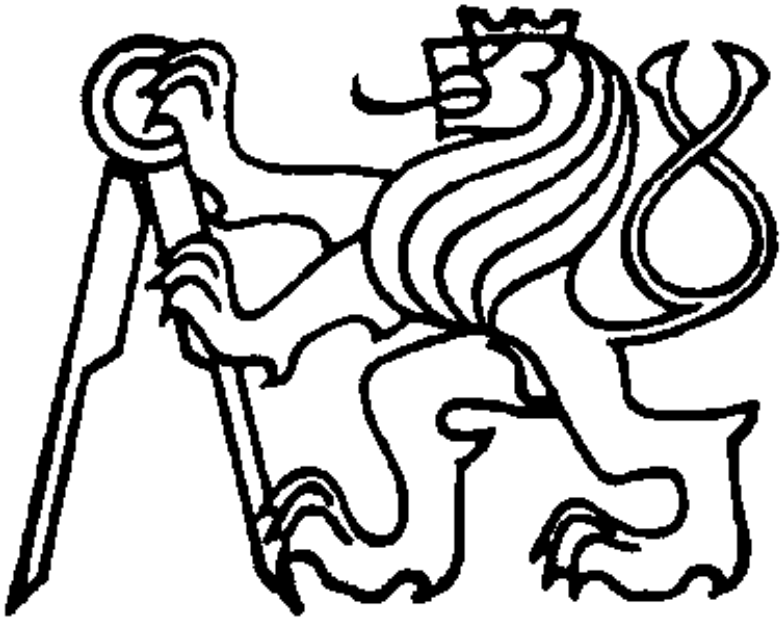

DOCTORAL THESIS STATEMENT

Czech Technical University in Prague

Faculty of Electrical Engineering

Department of Electrotechnology

João Vitor Bernardo Pimentel

ADAPTIVE SELF-LUBRICATING LOW-FRICTION COATINGS

Ph.D. Programme: Electrical Engineering and Information Technology

Branch of study: Electrotechnology and Materials

Doctoral thesis statement for obtaining the academic title of "Doctor", abbreviated to "Ph.D."

Prague, April 2013

The doctoral thesis was produced in full-time manner Ph.D. study at the Department of Electrotechnology of the Faculty of Electrical Engineering of the CTU in Prague

Candidate:

João Vitor Bernardo Pimentel
Department of Electrotechnology
Faculty of Electrical Engineering of the CTU in Prague
Technická 2, 166 27 Prague 6

Supervisor:

Tomáš Polcar
Department of Control Engineering
Faculty of Electrical Engineering of the CTU in Prague
Karlovo nám. 13, 121 35 Prague 2

Opponents:

.....

.....

.....

The doctoral thesis statement was distributed on: .....

The defence of the doctoral thesis will be held on ..... at ..... a.m./p.m. before the Board for the Defence of the Doctoral Thesis in the branch of study Electrotechnology and Materials in the meeting room No. ..... of the Faculty of Electrical Engineering of the CTU in Prague.

Those interested may get acquainted with the doctoral thesis concerned at the Dean Office of the Faculty of Electrical Engineering of the CTU in Prague, at the Department for Science and Research, Technická 2, Praha 6.

.....

Chairman of the Board for the Defence of the Doctoral Thesis
in the branch of study Electrotechnology and Materials
Faculty of Electrical Engineering of the CTU in Prague
Technická 2, 166 27 Prague 6.

Contents

1. Current situation of the studied problem

The study of the natural phenomena in tribology is relatively new in science, having benefited strongly with the development of advanced instrumentation in the 20th century. The study of tribology itself, as the interaction between surfaces in relative motion, is much older: we can consider for example that Leonardo da Vinci studied basic laws of friction in the 15th century. Still, the term *tribology* was only introduced as a new field of science in 1967, with its root in the Greek *tribos* for rubbing or sliding [1].

The importance of the tribological properties of mechanical systems is crucial nowadays: wear is the major cause of waste of material and degradation of mechanical performance, and friction causes not only wear but energy dissipation: about 30% of the energy resources in the world are spent on friction [2]. Besides, there are environmental issues associated with the disposal of lubricants used to reduce frictional losses.

This work is dedicated to the study of self-lubricant thin films for tribological applications. These films are deposited over the surface of a substrate, or bulk material, with the main purpose of enhancing (or adding) some properties to the composite system *substrate–coating* [3]. The coatings dealt with here are based on transition metal dichalcogenides (TMDs) doped with different elements.

1.1 Adaptive solid lubricant coatings

Self-lubricant films have been in focus for several decades for their potential use in aerospace applications, where devices face friction and wear in the contact of moving parts, low-frequency vibrations and high loads. These are, furthermore, repeated in extremely different conditions, e.g. from relatively high pressure and humidity on land, to low pressure and humidity in high altitudes. For such applications, it can be critically important to avoid using liquid lubricants [4]. Commonly used solid lubricants in space applications were transition metal dichalcogenides, deposited by spray or vacuum methods, applied as powders, or burnished. However, these materials (which have also been used successfully as additives for oil lubricants [5]) were soft and oxidized easily in air [4,6]. More advanced approaches were sought to develop solid lubricants that could perform well enough in different environmental conditions, leading to composites of oxides and

TMDs, and metal-doped TMDs [7,8]. Eventually, self-lubricant composites were developed which combined properties of solid lubricants and a supporting matrix whose structure and mechanical behaviour could change according to contact conditions to maintain low friction and wear. The most obvious advantage for aerospace applications was that, if a versatile coating exhibited good properties both in dry and humid atmospheres, the system needed only one type of solid (self-) lubricant.

Coatings that can adapt their properties to satisfy the requirements of the operating conditions are often called *adaptive* or *smart* coatings. The motivation for their use is not limited to environmental cycling: while the tribological performance of TMD-based films is particularly good in dry conditions, recent studies by Cavaleiro et al. [9] have shown that this type of coatings can exhibit very low friction in humid air as well, due to their adaptive characteristic.

1.2 Transition metal dichalcogenides (TMDs)

The films belonging to the class of transition metal dichalcogenides are composed of sulfides, selenides or tellurides of tungsten, molybdenum or niobium. TMD-based thin films exhibit unique properties based on the high degree of anisotropy in their structures, in a kind of lamellar nature similar also to that of graphite. It is the basis for the good lubricating properties of these materials, although they can differ in lubrication mechanisms [10].

The basic structure of the TMD is a hexagonal cell in which the metal sits in the middle of a "sandwich", the top and bottom being the chalcogen atoms. The bonds within the sandwich structure are strong, but the bonds between the chalcogens of adjacent cells are very weak van der Waals forces. Given a polycrystalline structure composed of such cells, if a contact partner slides in a plane parallel to that of the TMD layers, the bonds between cells are easily broken and the upper layers slide over the ones below. This *type I* configuration, with the basal planes of the crystallites parallel to the sliding surface, is favorable for low friction. If the basal planes are perpendicular to the sliding surface (*type II*), the self-lubricity is lost. It is still possible, however, that the sliding process moves or rotates the cells, so that the sliding itself causes a preferred orientation to appear on the surface [11].

The hexagonal structure of MoS_2 is shown in Fig. 1. Such configuration, referred to as 2H-MoS_2, is not the only possible phase for MoS_2; but since it is the most stable phase, it is usually referred to simply as MoS_2 [12].

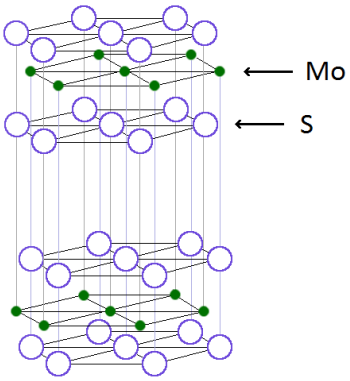

Fig. 1 Hexagonal structure of 2H-MoS_2 (adapted from [5]).

In vacuum or dry atmosphere, TMDs exhibit very low friction (even achieving superlubricity in ultra-high vacuum). TMDs are very susceptible to oxidation, particularly when the surface crystals are not in the preferred type I orientation [13]; but while this orientation leads to good self-lubricating properties, it also shows the worst adhesion to the substrate. A common problem of pure sputtered TMD films is the formation of columnar or porous structures in the material which can, among other problems, promote penetration of oxygen or water vapour. Water molecules can react with dangling bonds at the edge of the crystallites, hindering sliding of one layer over another and their reorientation. Oxygen reacts very easily, substituting atoms of the chalcogenide in the structure. Humidity in storage strongly enhances surface oxidation, although the process of sliding under a contact load can easily remove surface oxides and create a pure-TMD tribolayer [9]. It should be noted that in most TMD films deposited in vacuum (and in all those presented here) there is some percentage of oxygen in the as-deposited films, originating from the residual atmosphere in the chamber [14]. In our films, the use in deposition of very porous targets which had been stored in open air also contributed to oxygen contamination.

Another typical drawback of TMDs is their low load-bearing capacity. MoS_2 and WS_2 films typically have hardness values below 1 GPa. One way of solving this problem that has proved successful is alloying TMDs with other elements or compounds.

1.3 Doped TMDs

The introduction of dopant atoms in the deposition of TMD films prevents the formation of large TMD structures in the film (i.e. large grain sizes) and hinders columnar growth. In some cases the resulting structure is fully amorphous, e.g. in the case of Mo-S-Pb [8] or W-S-N coatings [9], reducing the occurrence of failures, improving adhesion and providing a level of protection

against contamination [15,16]. Furthermore, the more compact and denser structure improves the hardness of the film. Studies carried out at the University of Coimbra with tungsten disulfide (WS_2) alloyed with carbon and nitrogen showed increase of hardness by doping of one order of magnitude and higher [17]. These conclusions were validated in later studies [18,19]. The low friction observed, however, was not accounted for directly by increased hardness and density. It has been suggested that, besides the previous considerations, more disordered morphologies prevent long-range order of the TMD phase, thus decreasing the propagation of cracks on the film surface [13].

An alternative suggestion was that the dopant material, particularly in the case of carbon, would contribute actively to the decrease in friction – graphite would not only cause changes in morphology, but would also interact with the sliding partner with its own low-friction characteristics. This concept was summarized in what was called the *chameleon effect*: the idea that in dry conditions, these films would maintain the typical excellent tribological behaviour of TMDs, and in humid air, the good tribological properties of diamond-like carbon films (DLCs) would be predominant [20]. However, the hypothesis of the "chameleon effect" has not been supported by recent results. It seems more likely that the main contribution of dopants to the friction behaviour is related to facilitating the formation of a low-friction TMD tribolayer between sliding partner and coating. In other words, the role of carbon in friction is only indirect by increasing coating hardness and density. Polcar et al. [21] have shown that wear track analysis from sliding tests in dry and humid air presented no significant difference, and that in both conditions a TMD tribolayer was formed. Similar results were obtained during this work and are discussed in detail in the doctoral thesis.

In this regard, it should be noted that although all tungsten and molybdenum disulfides presented in this work were sub-stoichiometric (i.e., with deficiency in sulfur), they still exhibited S/W or S/Mo ratios above a level needed to maintain the self-lubricating properties. Moreover, for tribological testing, W/Mo disulfides were the most crucial components in the material and were in fact detected near the surface. For this reason, these coatings will be referred to as *doped TMDs* even when the TMD is not the major part of the chemical composition.

2. Aims of the doctoral thesis

The main purpose of the doctoral thesis was to expand our knowledge of self-lubricant adaptive coatings. After bibliographical research, the initial choice was made of the most promising types of doped TMD films for the objectives of this work. Different compositions and systems of sputtered self-lubricating adaptive coatings were studied, deposited, characterised, and tested. The thin films were based on molybdenum and tungsten disulfides or diselenides, doped with different elements (carbon, chromium, and titanium). The properties desired were improved hardness compared to undoped films, low friction, and high wear resistance – in humid air and without using liquid lubrication.

The research included systems that had already displayed good results in previous studies as well as systems that had not so far received much attention. Thus, this work involved the use of the current state-of-the-art at the same time as attempting to gain a deeper understanding of the mechanisms involved in the tribological behaviour of TMDs in general and the shared and differing characteristics of this class of coatings.

3. Working methods

Various systems of thin films based on tungsten and molybdenum disulfides and diselenides were deposited on steel and silicon substrates. The films were characterised using a range of different techniques and tested under varying conditions, which served to improve the properties of each system separately as well as to verify common characteristics of doped-TMD coatings. In some cases there was, to the best of our knowledge, no available literature dealing with the compositions tested.

Out of the eight systems studied, four had been deposited beforehand by colleagues at the University of Coimbra: molybdenum disulfide doped with carbon (Mo-S-C), molybdenum

diselenide doped with carbon (Mo-Se-C), tungsten disulfide doped with carbon (W-S-C), and tungsten diselenide doped with carbon (W-Se-C). All other depositions were carried out as part of the doctorate work.

The most important techniques used in the course of this work will be described briefly in the following sections. The main results obtained will be presented in Chapter 4, along with an overview of the common characteristics of the different systems.

3.1 Sputtering deposition

Sputtering is a method used either for cleaning surfaces or for physical vapor deposition (PVD). The target (solid) is placed in a vacuum chamber filled with an inert gas (typically Ar). By using a strong electric field, the gas is ionized and the plasma is generated. The electric field accelerates the ions in the plasma towards the target, hitting it with high kinetic energy; if the ions are accelerated enough, atoms are ejected from the target [22]. Magnetrons are used in deposition chambers to increase the probability that electron will ionize further gas atoms.

By placing the targets of the material to be deposited face to face with the substrates, atoms ejected from the surface of the target will reach the substrate with enough energy to adhere to (or be implanted into) the surface. With time, the substrate's surface will be coated with the material sputtered from the target. When more than one target is used (*co-sputtering*), the coating will be a combination of those materials.

During the sputtering process, there are a number of phenomena occurring at the same time. For example, Ar^+ ions and accelerated electrons may hit the substrate and eject atoms from the coating (*re-sputtering*); ions and electrons may hit the surface of the target without enough energy, only heating the surface locally; if the pressure is too high and the plasma too dense, the sputtered atoms may lose (by collisions) the energy needed to form a dense film. Furthermore, the incidence of re-sputtering and the different sputtering rates of different materials influence the ratio with which they adhere to the substrate. Thus, it can be seen that the final results of depositions depend not only on the materials being deposited but also strongly on the conditions inside the chamber and the deposition parameters.

Fig. 2 represents schematically a deposition chamber exemplifying the co-sputtering method used in this work; in the case shown, the deposition of WS_2 doped with C or C + Cr. The targets are made of chromium and carbon (graphite). Pellets of WS_2 are placed on the

erosion zone of the C target, i.e. on the area sputtered more intensely (due to the electromagnetic fields). For a given set of deposition parameters, the ratio between Cr and WS_2 + C in the coating can be controlled by the individual powers applied to the targets. The ratio between WS_2 and C, on the other hand, is controlled by the number of pellets. Finally, the S/W ratio on the film is sensitive to deposition conditions; re-sputtering, for example, is more likely to eject S from the substrate than W, since sulfur atoms are much lighter. The substrates are kept rotating above the targets so that they are constantly moving, passing above each target alternately and not staying above either target long enough for a multilayered structure to grow. The coatings deposited in the scope of this work were all deposited in such a way as to avoid multilayers.

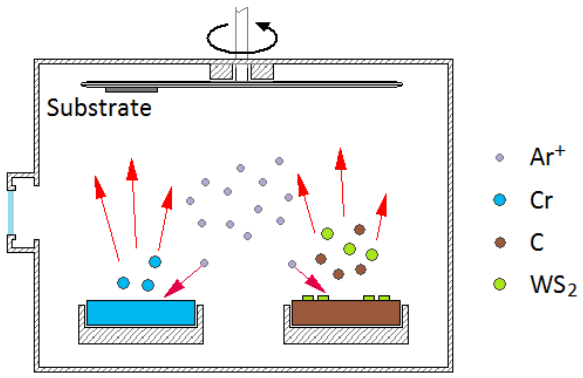

Fig. 2 Representation of a vacuum deposition chamber for magnetron co-sputtering.

3.2 Electron probe microanalysis

Electron probe microanalysis (EPMA) is a non-destructive technique used to determine the chemical composition of a material. The sample is bombarded with an electron beam, and so the material emits X-ray photons with wavelengths characteristic of its composing elements. The chemical composition of the sample can thus be determined [23]. For a quantitative analysis, it is assumed that the sample material is homogeneous. The intensity of the signal attributed to each element must be compared with a pre-established standard in order to determine its amount in the sample. Many factors can differ between the standard and the sample, so their effect can be thought of as a measurement background; that is why the atomic percentages obtained by EPMA often had to be corrected to add up to 100%. Unless otherwise stated, EPMA results presented here were weighed as a sum of the target elements, excluding oxygen, since surface contamination was inevitable.

3.3 Nanoindentation

Hardness values of the coatings were measured by depth-sensing indentation technique (nanoindentation). The indentation technique works by pressing a very hard tip into the coating, applying a controlled load, and measuring the depth of the penetration. If the properties of the tip are well known, then the area of the indentation produced on the coating can be calculated from only the penetration depth. Nanoindentation (essentially the same technique using small loads and depths) has become the predominant technique for hardness measurement of thin films [3]. The hardness values used in this work were always calculated from the average of at least 10 such measurements in 2 different locations on the surface of the coating.

3.4 Scratch test

Scratch tests were dedicated to evaluating the adhesion of the films to the substrate. The basic principle of the test is to move an indenter (a hard diamond tip) in contact with the surface of the coating, apply a load, and examine whether it causes the coating to present any failure (cracks, delamination, etc.) The *critical load* is determined as the load at which adhesive or cohesive failures start to occur in the coating. Scratch test results are greatly influenced by testing conditions, so values should be compared only within similar types of tests [24]. Most results in this work were averaged from several tests (between 2 and 4) performed in different spots, obtained with the load increasing linearly while the indenter moved across the surface at a rate of 10 N/mm. The scratches were then analysed under optical microscope and three-dimensional profilometer.

3.5 Ball-cratering test

The main method for evaluating the thickness of the coatings was the ball-cratering test (also called *calotest*). The test consists in rotating a steel ball with known diameter in contact with the coating, with an abrasive solution added to the contact. If the test is long enough, the ball wears through the coating and reaches the substrate, so that the resulting spherical cap is deep enough to wear the substrate as well. The thickness of the coating can then be calculated from a simple visual analysis of the worn cap. Thickness measurements using ball-cratering test were compared, when possible, with results from profilometry and SEM of cross-sections.

3.6 Sliding tests

Tribological tests were performed using a standard pin-on-disc tribometer. (Despite the name, the *pin* can be of different shapes; a ball is typically used because of its simple geometry.) The sample is fixed on a planar support which, ideally, rotates around a single axis. The pin is mounted on a lever, placed in contact with the sample, and a controlled load is applied (as illustrated in Fig. 3). The friction coefficient μ can then be determined by measuring the horizontal displacement of the lever arm. Its dimensionless value is given by $\mu = F / N$, where F is the frictional force, parallel to the sliding; and N is the normal force, exerted by the load. Most of the sliding tests presented were carried out at room temperature in humid air (relative humidity around 30%) using 6 mm 100Cr6 steel balls as static partners, and the values of μ used were the average of the entire test, unless stated otherwise.

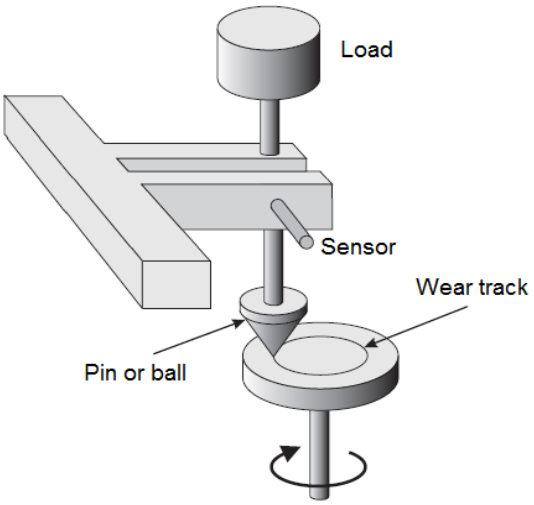

Fig. 3 Schematic of a pin-on-disc tribometer, adapted from [22].

By analysing the wear tracks produced during sliding tests, the wear rate can also be calculated. It is is usually expressed in $mm^3/N \cdot m$ – unit of volume per unit of load per distance. The total length of the test can be calculated simply from the perimeter of the wear track multiplied by the number of cycles, while the area of the cross section and the length of the track give us the (approximate) total worn volume. Wear rates of the pins were obtained by measuring the spherical cap and thus determining the worn volume.

3.7 Three-dimensional optical profilometry

The three-dimensional optical profilometer used is based on white-light interferometry. In this technique, a light beam is reflected on the surface of the sample, detected and compared with a reference beam. The topology of the sample leads to different path lengths of the reflected beam, which cause interference patterns to appear when the beams are combined and thus it is possible to characterise the surface [23]. With the equipment used, topological features of up to 200 μm could be measured, in a field of vision of up to 1.40 × 1.05 mm (however, adjacent areas could be combined to compose larger 3D profiles). The main limitation when analysing TMD coatings was the sensitivity to the reflected light. If the light intensity was too low, the device could not retrieve enough information about the surface. On the other hand, if the reflected light was too strong, the measurement saturated and again no useful data were retrieved. In regions combining spots of very different reflectivity, part of the data was inevitably lost.

3.8 Raman spectroscopy

Raman spectroscopy is a non-destructive characterisation technique where the sample is irradiated by laser beams in the UV–visible range. When scattered photons have wavelengths different from the incident beam (meaning that energy was absorbed or lost by the sample), the effect is known as Raman scattering [25]. The shifts in wavelength can be used for identification of substances, since they are specific for a material. Raman scattering is usually a very weak phenomenon and it is challenging to achieve high sensitivity. Using high laser power is usually better, but the measurement parameters need to be adjusted for the sample under testing in order not to cause structural changes in the material under test. In practice, longer acquisitions can compensate low power, but also increases noise and the probability of interference by cosmic rays, which cause high-intensity narrow spikes to appear in the spectrum [26].

Associated with other analyses, Raman spectroscopy helped evaluate several properties of the deposited films. The appearance of characteristic peaks in the spectra helped evaluate the ratios of certain materials in the sample. Additionally, Raman spectra conveyed information regarding the crystallinity of the material, since more amorphous materials exhibited comparatively broader peaks.

3.9 Electron microscopy

Scanning electron microscopy (SEM) is a surface characterisation technique that allows imaging of the topography of a surface with high lateral resolution [22,23]. The probe (a focused electron beam) scans the surface of the sample. The microstructural information collected is provided mainly by the inelastic scattering processes due to the interaction between probe and surface. The major source of data is usually secondary electrons emitted when the electron beam hits the surface. Since they have low energies, only those close to the surface are detected.

SEM measurements presented in this work were obtained either perpendicular to the direction of film growth, thus analysing the cross section, or on the surface, to evaluate its topography. The technique called *Energy Dispersive X-ray* spectroscopy (EDX or EDS) was also used in this work to evaluate material composition (similarly to EPMA), using the same equipment as SEM measurements, but working with a different range of signals.

Transmission electron microscopy (TEM) works similarly to SEM, but the electron beam goes through the sample, which must be thin enough (typically below 0.1 μm) for the electrons to pass without serious energy loss. The electron beam in TEM has higher energy, resulting in resolution high enough to image planes in a crystal lattice. Information is acquired from primary electrons emitted by the beam and their elastic collisions with the sample. Since the electrons detected are all supposedly emitted with same energy and same acceleration, the resulting image is directly related with the material structure [22].

3.10 X-ray diffraction (XRD)

X-rays can convey information about a crystal structure if their wavelength is comparable to the size of the geometrical variations in the material [23,27]. The diffracted rays coming from the surface may interfere constructively or destructively with the rays coming from inner layers, therefore the intensity of the outgoing rays will depend on three factors: the wavelength of the X-rays, the angle of incidence, and the distance between the planes. Thus, data from XRD spectra provide information about the structure of the material (and in the case of thin films, possibly the substrate as well, since X-rays can penetrate microns into the sample [22]). Besides, small grain sizes, crystal lattice faults, and randomly-oriented grains cause broader peaks in the spectra than the sharp, intense peaks resulting from single-crystal and oriented structures.

3.11 X-ray photoelectron spectroscopy (XPS)

XPS was used in this work mainly to analyse chemical bonding. The technique is also based on exposing the sample to X-rays: the monochromatic photons in the incident beam are absorbed by the atoms in the sample, which ejects secondary electrons with energy equal to the difference between the energy of the incident photon and the energy needed to displace the secondary electron [22]. The secondary electrons are detected, and the intensity of the signal over a range of corresponding binding energies composes the XPS spectrum. Changes in the chemical environment of the atom will influence the binding energy, so that photoelectronic emission from the same element in different binding states will generate (slightly) different peaks. Electrons emitted in layers deep within the material have small chance of reaching the surface and being detected, so this technique characterises only the few uppermost atomic layers [22,23]. Consequently, surface contamination strongly influences the results, and usually the sample is sputtered with ions prior to measurement.

---

4. Results

In this Chapter will be presented the main experimental results obtained, starting with an overview of the deposition, chemical composition and mechanical properties of the different systems of films. We then present a few important points of their characterization and analyses, organized by their composing elements (i.e. base TMD and dopants). Details and a discussion of important results can be found in the thesis.

Different coatings in the same systems will often be referred to by their dopant atomic percentage followed by the dopant symbol; e.g. a Mo-S-C film with a carbon content of 34 at.% will be referred to as *34C* when compared with others in the same series.

4.1 Deposition and chemical composition

The relation between dopant content in the films and the power ratio of the targets during deposition was nearly linear for almost all systems in this work (with the exception of W-S-C, where the composition was not varied). The case of Mo-S-C is shown in Fig. 4. Mo-S-C films were deposited by r.f. magnetron co-sputtering from two targets, MoS_2 and C (graphite). The carbon content in the samples was varied up to 55 at.% C by varying the power ratio P_C/P_{MoS2} – i.e. controlling the power applied to each target individually. The deposition rate decreased with increasing C content since the sputtering yield of MoS_2 is much higher than that of C. Deposition times varied considerably in all systems deposited, due to different sputtering yields. All films presented in this work were between 1.2 and 3.8 μm thick.

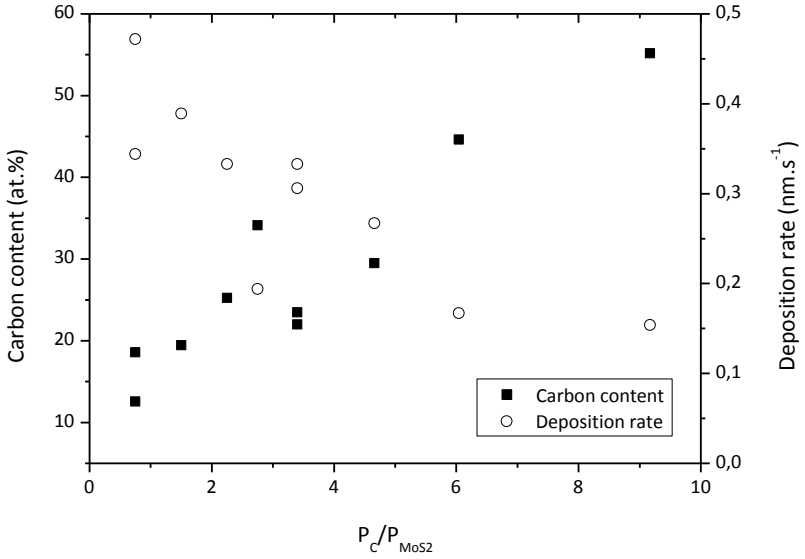

Fig. 4 Carbon content and deposition rate as a function of C/MoS_2 target power ratio.

The depositions of W-S-C-Cr, W-S-C-Ti and Mo-S-C-Ti were carried out using two targets (one graphite and another Cr or Ti) and TMD pellets, as described in section 3.1. The number and distribution of pellets on the graphite target was kept fixed throughout different depositions in one series; nevertheless, EPMA results showed that when the target powers changed, there were variations in the C/TMD ratio, as well as in the S/M ratio (*M* = Metal, i.e. either molybdenum or tungsten). This was attributed mainly to re-sputtering (see section 3.1).

EPMA results showed moreover that the deposition process is repeatable by using the same parameters. The chemical composition of W-S-C-Cr coatings is shown in Table 1 (where i, ii, iii denote different depositions).

Table 1 Chemical composition of W-S-C-Cr coatings

Deposition		Chemical composition (at.%) - EPMA				
		W	S	C	Cr	O
0Cr		23.6	29.8	42.0	0.6	4.2
7Cr	i	20.3	25.1	40.4	7.0	7.2
	ii	19.1	26.6	38.2	7.0	9.1
13Cr	i	17.4	23.0	37.7	13.4	8.5
	ii	18.5	24.1	35.8	13.5	8.1
	iii	18.2	22.4	38.1	13.5	7.8

Prior to all depositions carried out in the scope of this work, the following standard procedures were adopted: the steel substrates prepared for deposition were polished with 3 μm-grain diamond solution. All substrates were cleaned in ultrasound submerged in acetone and in ethanol. The substrates were then dried and placed in the deposition chamber. They were later sputtered with Ar^+ ions before the start of the deposition.

4.2 Hardness

A common drawback of TMD films is the typically low hardness. The doped TMD-based films presented showed improvements over pure TMDs, resulting in hardness values of up to 9 GPa. Increasing the dopant contant led to a corresponding increase of hardness values in almost all compositions in this study. One exception was the case of tungsten disulfide doped with chromium. Unlike in the other systems presented in this work, hardness values of W-S-Cr films did not show any direct relation to chemical composition. However, the effect of the pressure in the chamber during deposition was evident. The majority of the W-S-Cr coatings were deposited in pressures lower than ~4.5×10^{-3} mbar and exhibited hardness around 7.4 GPa, regardless of Cr at.%. Those deposited in higher chamber pressures displayed hardness values below 3.5 GPa (see Fig. 5).

The hardness of tungsten disulfide films alloyed with carbon and chromium (W-S-C-Cr) was between 4.9 and 7.2 GPa (always higher than that of pure WS_2) and the critical load between 12 and 23 N. In both cases, the values increased with Cr content (see Fig. 6). Investigation by TEM of a W-S-C film had revealed randomly oriented and separated WS_2 platelets dispersed in the carbon matrix [18], which could slip easily and reduce hardness. Alloying W-S-C with Cr could therefore transform nanostructured films into amorphous material, as was verified by TEM (see

Fig. 7) in a series of analyses performed by the Applied Materials Science group at the Department of Engineering Sciences of Uppsala University, Sweden, and published in Ref. [28].

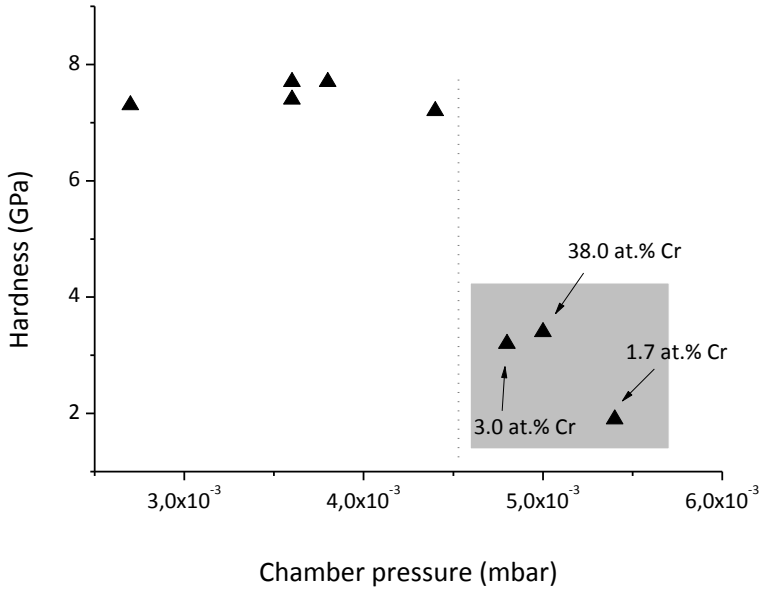

Fig. 5 Relation between pressure during deposition and the achieved hardness of W-S-Cr films.

Nanocomposite W-S-C films with hard tungsten carbide nanograins embedded into an amorphous carbon matrix can exhibit hardness above 10 GPa. While our W-S-C-Cr coatings were still significantly harder than pure WS_2 films [4,29], there was no conclusive evidence of WC grains. The analyses of microstructure and chemical bonding of the other coatings presented in this work have also strongly suggested that the improvement in hardness (and adhesion) observed should be attributed only to the densification of the material and the prevention of porous and large crystalline structures in the films.

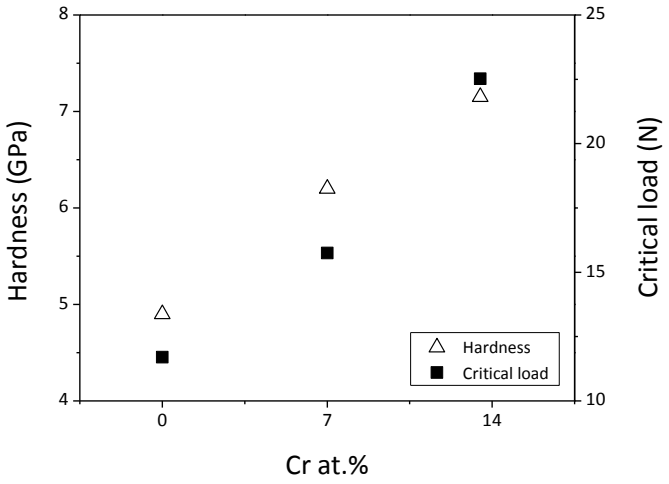

Fig. 6 Hardness and critical load for different Cr contents of W-S-C-Cr films.

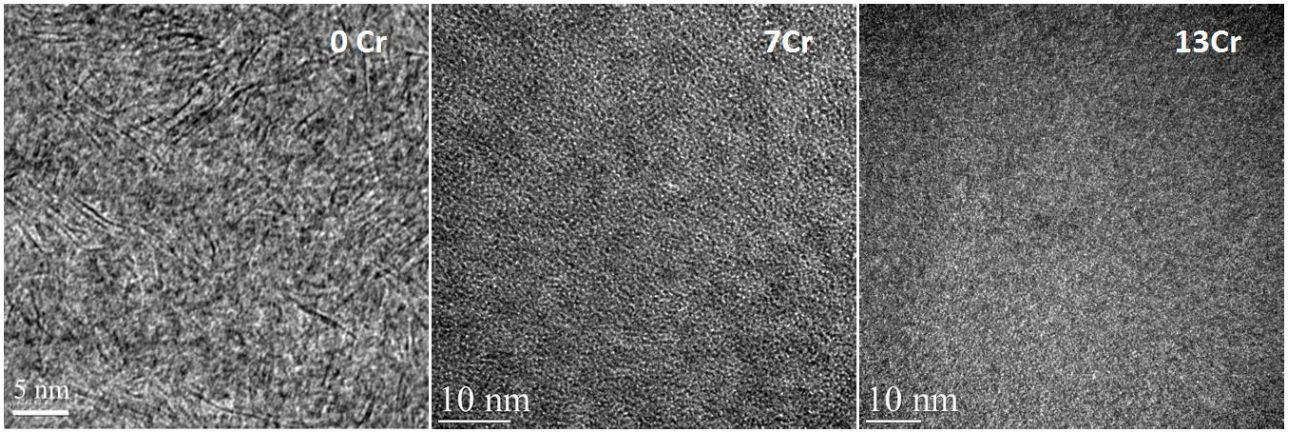

Fig. 7 TEM images of different compositions of W-S-C-Cr films (adapted from [28]).

4.3 Mo–S–C (molybdenum disulfide doped with carbon)

Part of the content in this section has been published in the paper:

> J.V. Pimentel, T. Polcar, and A. Cavaleiro, "Structural, mechanical and tribological properties of Mo-S-C solid lubricant coating", *Surface and Coatings Technology* vol. 205 (2011), pp. 3274-3279.

A large number of different compositions of Mo-S-C had been deposited. The characterisation and testing of the Mo-S-C films and wear tracks was focused on evaluating changes due to the varying composition.

4.3.1 Analysis of the as-deposited surfaces

In the Raman spectra of the films, there were two evident pairs of peaks, the first corresponding to MoS_2 (at approx. 370 and 410 cm^{-1} [30]), and the second to the D and G peaks of carbon (at approx. 1420 and 1560 cm^{-1}) that usually appear in the spectra of carbon-based coatings [31]. The ratio of the peak areas I_C/I_{MoS2} showed a direct relation to the ratio of deposition powers, P_C/P_{MoS2}. Fig. 8 shows Raman spectra for different carbon content and the relation between power ratio and peak ratio (in the inset). It can be seen also that the MoS_2 peaks became broader for higher C content, an evidence of more amorphous structure. There was no significant indication of structural changes in the carbon matrix.

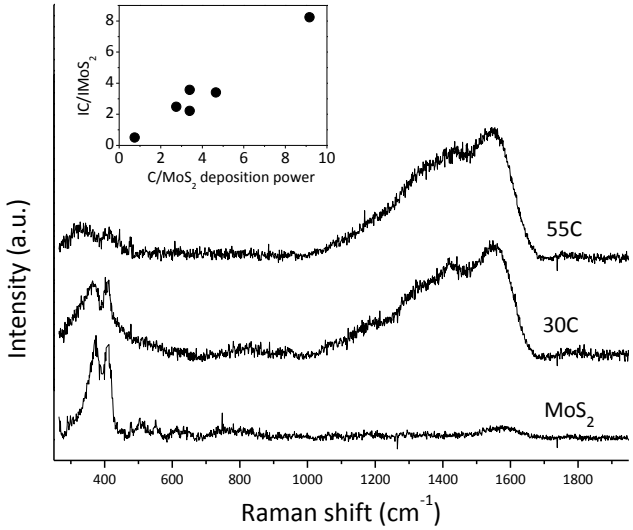

Fig. 8 Selected Raman spectra of Mo-S-C films.

4.3.2 Tribological properties

Tribological tests were performed in humid air with various loads (up to 30 N). For low carbon content (below 30 at.%), the running-in process was characterised by high friction coefficients which later decreased to lower stable values (steady state). The trends differed in high C content coatings. Fig. 9 shows friction curves for different compositions under the same conditions. The coating with the highest carbon content showed the lowest friction and the lowest wear rates for both the coating and the counterpart. There was a wide variation of wear rates among the different compositions, from 0.28×10^{-6} to 16.6×10^{-6} mm^3/Nm (for 55C and 23C, respectively). The films showed relatively low adhesion, and in some cases adhesion failures occurring during sliding probably led to higher friction and wear. These failures did not provoke immediate increase of friction, however, due to the self-lubricating characteristic of the films and material attached to the ball. The adhered tribolayer in the center of the ball was very thin, but wear debris composed of Mo-S-C was found to be accumulated behind the wear scar.

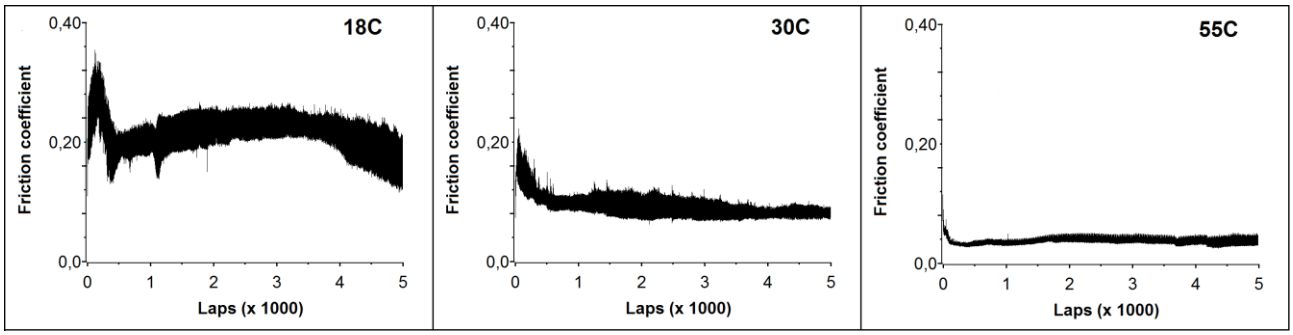

Fig. 9 Selected friction curves for different compositions under 18 N in humid air.

4.4 W–S–C (tungsten disulfide doped with carbon)

Part of the content in this section has been published in the paper:

> J.V. Pimentel, T. Polcar, M Evaristo, and A. Cavaleiro, "Examination of the tribolayer formation of a self-lubricant W–S–C sputtered coating", *Tribology International* vol. 47 (2012), pp. 188-193.

The W-S-C films chosen for testing had a carbon content of 42 at.% and an S/W rate of 1.26, with hardness of 9 GPa and critical load higher than 9 N (an improvement over pure WS_2 films [29]). The films were tested with a focus on the effects of sliding on the coating material, such as the influence of different loads on the changes caused on the surface of the wear tracks.

4.4.1 Tribological testing

Three main sets of tribological tests were performed. The first set consisted of 5000-cycle tests, each with a different contact load in the range 1.0–50.8 N. In the second set, the load was constant (5 N), but the number of cycles varied from 100 up to 50000. The third set was actually a special procedure during a single tribological test: the rotation of the sample was paused every few laps and Raman spectroscopy was performed on the wear track. This was done in order to get a better understanding of how friction mechanisms evolve during sliding, and required an external lens connected to the Raman spectrometer via optical fiber. In such a way, we could consider Raman spectra as a *quasi in-situ* identification of the structural changes in the wear track.

Tests with varying load permitted a qualitative and quantitative analysis of the influence of the contact pressure. Increasing load led to lower friction coefficients, as expected for TMD-based films: the contact pressure during sliding should promote the orientation of the material close to the surface and the formation of a tribolayer, as referred to in Chapter 1. It is interesting to note that a coating composed only of amorphous carbon typically exhibits the opposite trend (i.e. higher friction for higher load [19]), which already suggests that the frictional behaviour in C-doped TMD films is determined mostly by the properties of the TMD. The results obtained (see Fig. 10) fit a logarithmic relation reasonably well. Polcar et al. [18] proposed the equation $\mu = AL^B$ to describe the dependence of friction with contact load (L) for W-S-C films deposited by r.f. magnetron sputtering. In the equation, the constant A relates to the material and contact conditions; B relates to the length of the test, in particular the changes in the coating and

formation of a third body due to repeated laps. In the present case, the experimental data fit the equation well with A = 0.19 and B = -0.46. Wear rates were low and also decreased with load (see Fig. 11). SEM analyses and 3D profilometry showed smooth and shallow wear tracks produced by lower loads. For higher loads, they became rough and deeper.

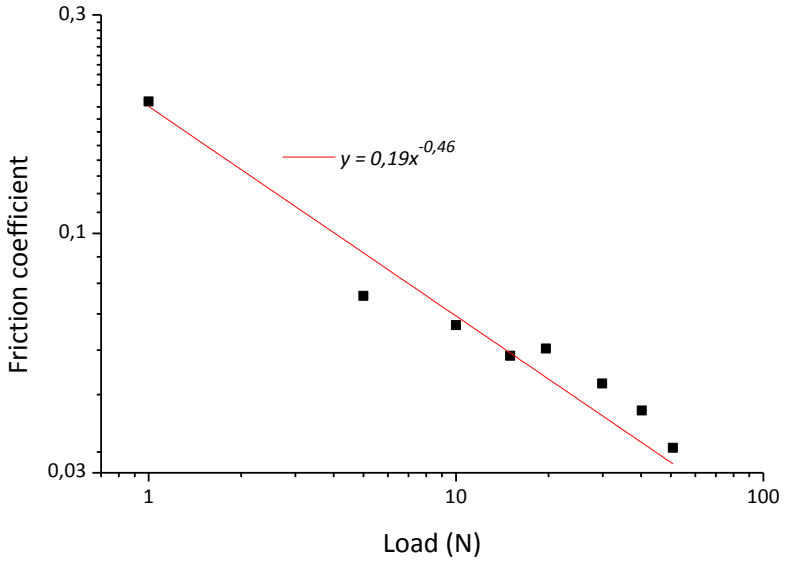

Fig. 10 Friction coefficient versus contact load.

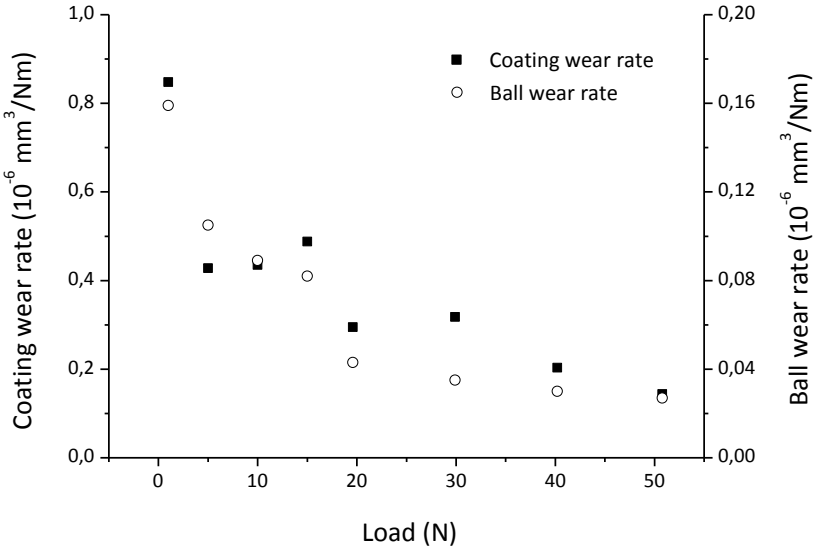

Fig. 11 Wear rate versus load.

High μ values occurred in the first laps, then dropped to a lower level, and afterwards stabilized in a steady-state regime. This stabilization happened much faster for higher loads (see Fig. 12). Moreover, in longer sliding tests it was possible to observe that the friction coefficient remained constant in the steady state till approx. 10 000 laps, when it started to increase.

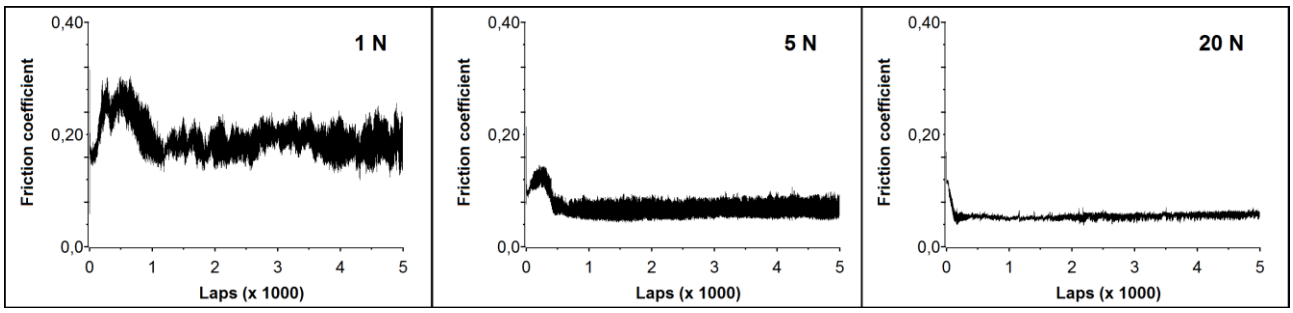

Fig. 12 Selected friction curves of W-S-C coating from sliding tests under different loads.

4.4.2 Structural analysis

X-ray microdiffraction was used in the analysis of the as-deposited surface and two wear tracks (see Fig. 13), to verify whether sliding caused significant structural changes. The broad peak at 34° with a broad shoulder extending to higher values indicated a turbostratic stacking of (10*L*) planes, where $L = 0,1,2\ldots$, as observed by Lévy et al. for WS_2 and MoS_2 [32]. This was a common feature in the XRD spectra of our films. There were no visible vestiges in the spectra of (002) orientation in the wear track, which would represent the reorientation of the basal planes to a type I configuration, as observed by Hirvonen et al. for pure MoS_2 [33]. They also observed a densification of the material and a consequent increase in hardness values inside the wear tracks. For our films, hardness measurements were carried out both on the as-deposited surface and on wear tracks, but no significant difference was found. It is likely that, since our coatings were already dense in the as-deposited state, re-orientation caused by the sliding process was only superficial and did not affect the mechanical properties of the film.

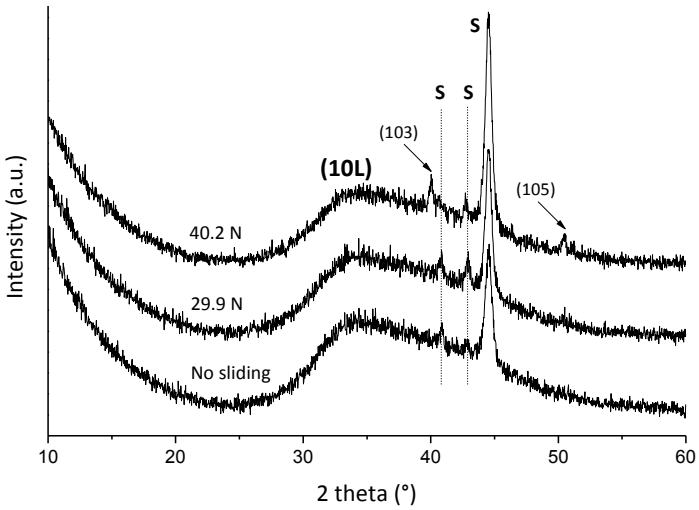

Fig. 13 Selected XRD spectra of W-S-C film surface and wear tracks produced under different loads. Peaks indicated by *S* originated from the substrate and are not relevant to our analysis.

Tungsten carbides could not be identified or ruled out from the XRD spectra due to the overlapping of peak positions, especially since small grain sizes would be expected [15]. XPS analysis was also inconclusive: the spectra in the W4*f* region fit well with doublets attributed to W–S and W–O bonds (see Fig. 14), so there was no need to assume any significant contribution of peaks corresponding to W–C bonds, which would appear in the same region [34].

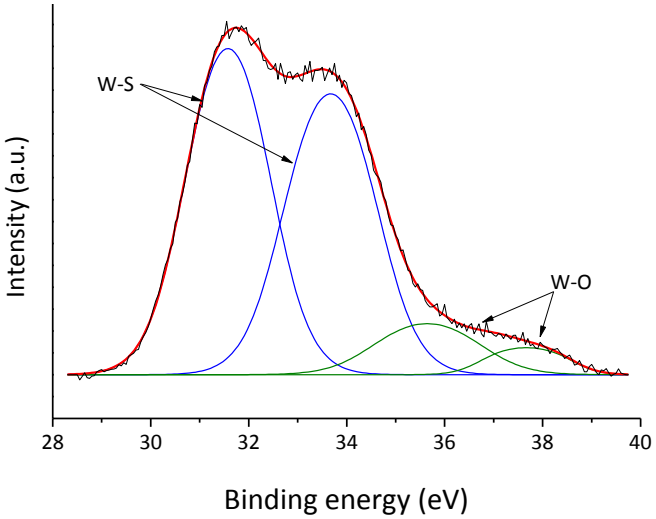

Fig. 14 XPS peaks acquired on the free surface in the W4*f* region

4.4.3 Raman spectroscopy

Raman spectra of WS_2-based films doped with carbon were characterised by two main regions of interest: peaks corresponding to WS_2 that appeared at approx. 307 and 421 cm^{-1}; and carbon D and G peaks, described earlier. Raman spectra were acquired on the free surface and on different positions inside wear tracks produced by 5000-lap tests. The ratio I_C/I_{WS2}, of the total area of C peaks divided by the total area of WS_2 peaks, varied significantly with the acquisition position (as shown in Fig. 15), decreasing progressively from the free surface (*I*) towards the centre of the wear track (*IV*). These results evidenced the formation of a WS_2-rich tribolayer and the influence of the contact pressure.

Spectra acquired in the centre of wear tracks produced by tests of different lengths revealed an immediate drop in the I_C/I_{WS2} value with test length, which increased slightly for longer tests. To better examine the changes occurring in running-in, *in situ* spectroscopy was carried out as described. Both the I_C/I_{WS2} peak ratio and the friction coefficient decreased rapidly at first (see Fig. 16), starting to increase monotonically after about 100 laps. The results confirmed

the polishing of the surface and material transfer in the beginning of the sliding process, supporting the idea that the formation of a WS_2-rich tribolayer takes place in these first laps.

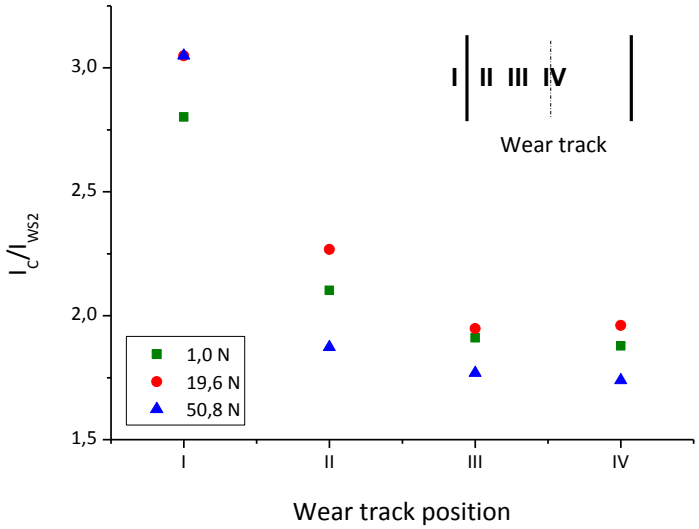

Fig. 15 Raman peak ratios according to position in the wear track.

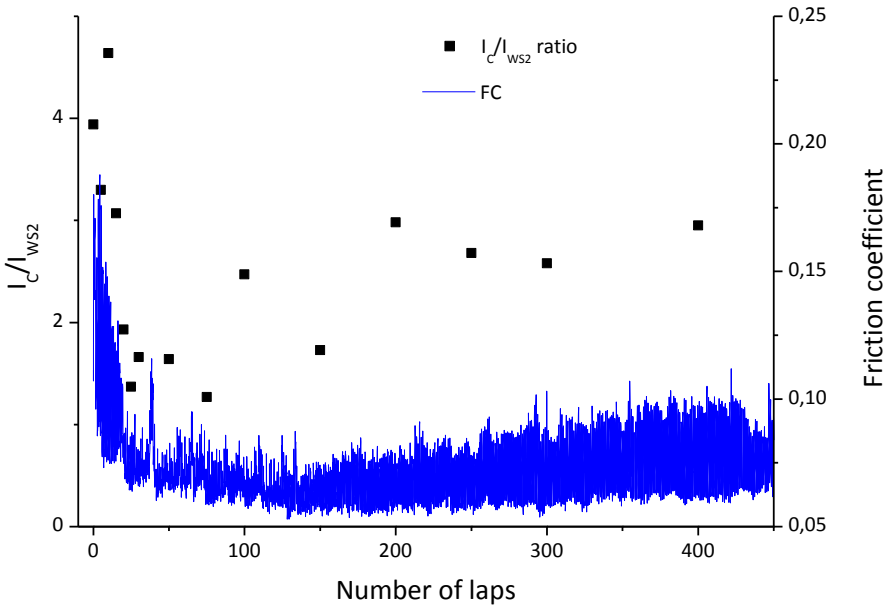

Fig. 16 Raman peak ratios and friction coefficient during running-in.

4.5 W–S–Cr (tungsten disulfide doped with chromium)

The W-S-Cr coatings selected as viable for more extensive testing exhibited tribological properties similar to other TMD-based systems. Although there was no significant relation between average friction coefficient and Cr content, the running-in process was much faster (less than 100 laps)

for films with higher dopant content, as was observed with Mo-S-C films. The wear rate of W-S-Cr coatings was about one order of magnitude higher than that of W-S-C. It is therefore not surprising that few of the compositions survived 5000-cycle tribological tests under 5 N.

4.5.1 Microstructure and chemical bonding

XRD spectra indicated amorphous films, with the dominant feature being a broad elevation related to stacking of planes. SEM measurements, although carried out in this case with low resolution, showed no visible columnar or porous structure (see Fig. 17).

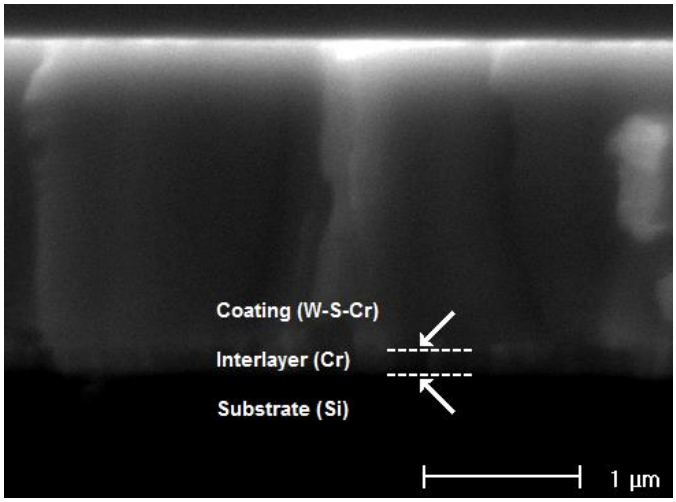

Fig. 17 SEM image of cross-section of the W-S-Cr coating with 29 at.% Cr.

The Raman spectra of W-S-Cr films did not show the characteristic "double-peaked" shape expected. The distortion of the region between ~230 and 450 cm^{-1} was attributed to two causes: the low crystallinity of the material, and the overlapping of peaks related to WS_2 and Cr oxide [35]. This was supported by the presence of a sharp peak at 475 cm^{-1} associated with Cr_2O_3.

4.6 W–S–C–Cr (tungsten disulfide doped with carbon and chromium)

Part of the content in this section has been submitted to *Surface and Coatings Technology* in March, 2013, as:

> J. V. Pimentel, M. Danek, T. Polcar, and A. Cavaleiro, "Effect of patterned surface on the tribology of W-S-C/Cr self-lubricant coatings."

The substrates used for deposition of W-S-C-Cr coatings included steel substrates with different patterns of grooves produced by micromachining. The investigation involving surface patterns was focused on their effect on steel substrates covered by a relatively thick self-lubricant coating – in particular, to verify the effect of the rough patterning on the coating's tribological performance. It has been shown that patterning surfaces can facilitate sliding, but unlike in the present work the most usual approach found in literature is to create cavities and grooves in a coating and then fill them with either liquid or solid lubricants [36].

Six different patterned substrates, labeled *A* to *F*, were prepared (see diagrams in Fig. 18). Groove widths were between 45 and 170 μm. All patterned substrates were coated with the 13Cr composition. Three-dimensional profilometry on selected spots on the grooves, before and after deposition, showed that the coatings copied the surface features of the substrates.

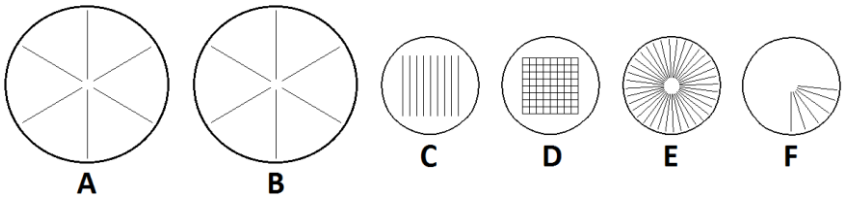

Fig. 18 Different patterns on the prepared samples.

4.6.1 Chemical bonding

XPS results were very similar to those of W-S-C films, although in this case W–C peaks had to be added to achieve an adequate deconvolution (according to conditions suggested in Ref. [37]). Indications of W–C bonds were also found in the C1*s* region. The spectra of the Cr2*p* region pointed to the possibility of having Cr bonded to C, S and W; not surprising when considering the amorphous nature of the films. Nevertheless, comparing spectra of films with and without Cr, it appears the alloying of W-S-C with Cr did not change the bonding state of the film.

Raman spectra of Cr_2O_3 usually show a pair of weak peaks at approx. 305 and 350 cm^{-1}, positions very close to WS_2. With the increase of Cr content, the region was distorted and only vestiges of WS_2-related peaks could be made out (see Fig. 19). One reason for this could be Cr_2O_3 and WS_2 peaks overlapping, but there was barely any evidence of other Cr_2O_3-related features. The change in shape was more likely related to structural defects and/or stress gradients in the volume. Moreover, the I_D/I_G ratio, an indication of disorder in the material [31], also increased with Cr content; the results therefore agreed with TEM observations (see section 4.2).

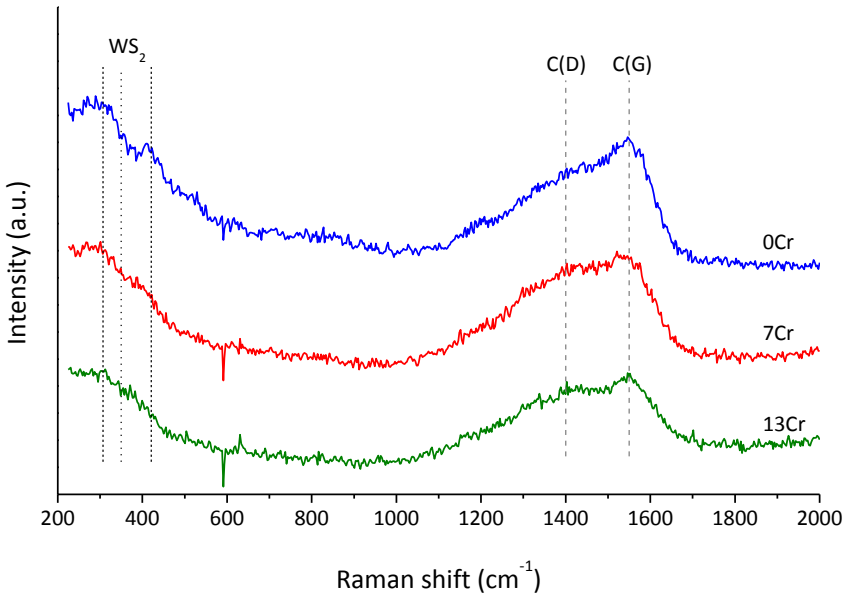

Fig. 19 Raman spectra of as-deposited W-S-C-Cr coatings.

4.6.2 Tribological properties of non-patterned samples

Pin-on-disc tests in humid air were carried out with varying loads (1–15 N) and test lengths (1000, 5000 and 50 000 cycles). The results agreed with those obtained with other series. Wear rates were generally higher for higher Cr content (see Fig. 20). The coatings survived endurance tests (50 000 cycles) without problems, exhibiting wear rates very similar after 5000 or 50 000 cycles. These results indicate that the majority of the worn volume is produced during initial stages of sliding, whereas wear is very low in the steady-state regime. Moreover, tests using *in situ* optical monitoring (an adaptation of the system used for *in situ* Raman spectroscopy) showed that the width of the wear track after 100 laps was approximately 95% of the width after 500 laps.

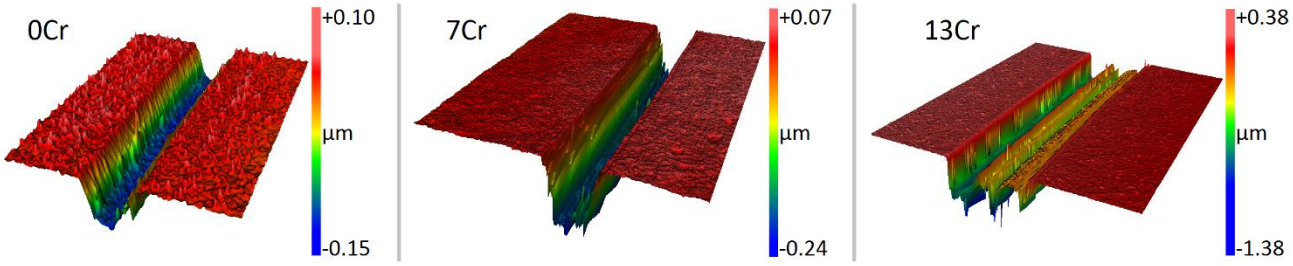

Fig. 20 3D images of wear tracks for W-S-C-Cr coatings with different compositions.

An investigation of the wear tracks indicated that the tribolayer was mostly amorphous tungsten and chromium oxide with small areas containing WS_2 platelets. A thin layer of (002) oriented WS_2 was found below the surface, at the interface between the coating and the tribolayer [28].

4.6.3 Tribological properties of patterned samples

Grooves on the surface significantly affected the tribological behaviour of the coatings. The friction coefficient of the reference non-patterned sample was 0.11; that of patterned samples C–F was overall higher, above 0.15, with the highest value of 0.20 observed for the sample with the highest density of grooves. However, the friction coefficients of samples A (0.10) and B (0.09) were slightly lower than the reference. During running-in on sample A, transitions in the friction curve matched the surface pattern but disappeared in the steady-state, when friction was more stable. 3D profilometry revealed that the grooves were completely filled up in the wear tracks and that wear was significantly lower immediately after the grooves, slowly increasing back up. Raman spectra indicated that the grooves were gradually filled with tribomaterial during running-in and thus acted as a reservoir of self-lubricating material, decreasing friction and wear.

The different groove patterns allowed for a complex comparison of their effect on friction and wear. The high friction of densely patterned films was comparable to that observed during the first cycles of sliding tests, drawing a parallel to a hypothetical extreme roughness, such that the initial polishing of asperities was never completed. The positive effect of surface patterns was thus limited to widely spaced grooves; otherwise, the low-friction tribolayer could not be formed. Wear depended mostly on their width and spacing, besides load and linear speed. With more experimental data and detailed analysis it should be possible to model the distribution and width of grooves that improve the tribological behaviour of a given self-lubricant coating.

4.7 TMD coatings doped with carbon and titanium

Two series of Ti-doped coatings were deposited, based either on W-S-C or Mo-S-C. In general, the films exhibited low adhesion and limited tribological performance: none of the coatings were able to sustain sliding tests for more than 25 000 cycles. There was no apparent relation between Ti content and friction coefficients. The original idea behind the incorporation of reactive metals such as Cr and Ti was that it was expected to protect the pure TMD phase from oxidation [38]. However, other authors have observed the deterioration of the wear resistance of Ti-doped TMD coatings, particularly associated with high Ti content; it has been suggested [39] that this is due to the formation of hard metallic titanium nanoparticles.

4.7.1 Chemical bonding and microstructure

Raman spectra were analysed to look for indirect indicators of carbide formation, but no evidence was found. XRD spectra showed the usual features – broad asymmetric peak indicating (10*L*) planes – for low-Ti films. When the Ti content increased, however, there was the predominance of peaks, albeit weak and broad, matching the diffraction angles corresponding to TiC. The evolution of the XRD spectra suggested therefore that the co-deposition with Ti led to the formation of TiC grains in the films, although in low structural quality.

4.8 Coatings based on molybdenum and tungsten diselenides

In literature, TMDs based on diselenides have shown tribological performance comparable with that of disulfide-based TMDs, besides being more resistant to humidity and high temperatures, and exhibiting higher hardness when doped with carbon [40]. However, the performance of the diselenide-based films examined in this work was seriously hindered by low adhesion to the substrates. The coatings used had been deposited beforehand, either by co-sputtering C and Mo/WSe_2 or by reactive sputtering of WSe_2 in a CH_4 atmosphere.

Most of the Mo-Se-C films tested exhibited severe adhesion failures and did not withstand sliding tests under the usual conditions – the only exception being 14C (friction coefficient: 0.1). The wear track produced was rough with indications that the coating was locally worn out in many spots. No further tribological tests were carried out on this Mo-Se-C series.

4.8.1 Tribological testing of W-Se-C coatings

After preliminary analysis, four compositions of W-Se-C were selected: two films prepared by co-sputtering (with 36 and 69 at.% C) and two by reactive sputtering (with 26 and 68 at.% C). Hardness was lower than for the other systems studied and very few films survived the usual sliding tests, therefore milder conditions were tried: pin-on-disc under 1 N load for 500 cycles. Under these conditions, the coatings with higher C content exhibited higher friction coefficients.

In order to verify if the W-Se-C coatings also exhibited decrease in friction with increasing load as observed in other systems, an alternative approach was used: tests under constant load using balls of different diameters (6.0, 7.94, and 10.0 mm). The contact pressure was thereby

lower with larger contact areas, so that friction was expected to increase with larger diameters (i.e., lower contact pressures). This was verified only in some of the tests. The main issue here was that the tests had to be so short that they probably did not span the entire running-in period before the coating was worn out. For the same reason, our assumption that the contact area is proportional to the size of the ball may not be valid until further stages of the sliding process.

Conclusion

Solid lubricant coatings based on doped TMDs were deposited and tested. Characterisation was carried out using several experimental techniques, among them new methods and innovative approaches. The films presented in this work were among the first to be analysed in our group's 3D optical profilometer and Raman spectrometer; they were furthermore the only ones so far to be examined with the equipment adapted for video monitoring and *quasi in-situ* acquisition of Raman spectra. These approaches undoubtedly yielded important results in our analyses, and also revealed plenty of room for improvement in handling these techniques and equipment.

An interesting point observed was the correlation between target power ratios, chemical composition, and Raman peak intensities. Although their interdependence was not thoroughly quantified, it is clear that these factors are almost linearly related. This is an interesting observation from an experimental point of view, since it suggests that a) given certain conditions, the chemical composition of doped films could be controlled by a single deposition parameter; and b) changes in the film material, such as observed during sliding, could be observed using a relatively fast and non-destructive technique, without restrictive measurement requirements.

We were able to verify common traits among the different compositions which helped elucidate the characteristics of tribological TMD films in general. A comparison of the main properties assessed in our analyses is presented in Table 2 (for medium dopant content). Friction coefficients are presented for tests in humid air, under 5 N for 5000 cycles.

Table 2 Comparison of results obtained with different series.

Composition	Deposition method	W or Mo at.%	S at.%	C at.%	Ti or Cr at.%	Hardness (GPa)	Friction coefficient	Critical load (N)
W–S–C	d.c. co-sputtering	26	32	42	--	9.0	0.073	9.0
W–S–Cr	d.c. co-sputtering	27	35	--	38	3.4	0.108	n/a
W–S–C–Cr	r.f. co-sputtering + pellets	20	24	41	15	7.2	0.107	22.5
W–S–C–Ti	r.f. co-sputtering + pellets	17	19	45	19	6.5	0.088	7.0
Mo–S–C–Ti	r.f. co-sputtering + pellets	18	25	44	13	5.7	0.117	< 4.0
Mo–S–C	r.f. co-sputtering	17	28	55	--	4.0	0.088	< 8.3

The characterisation and analyses of the films permitted a further understanding of their properties and the mechanisms involved in sliding, including the role of the dopants on the increase of hardness and on the formation of a low-friction tribolayer. The films exhibited improvements in load-bearing capacity and tribological properties in comparison with pure TMD films, particularly in humid air. The evolution of the sliding process was examined, as well as the effect of the contact load and other test parameters. Although the process is not yet fully understood, it seems clear that the self-adaptation of these films, promoting reorientation as a response to sliding, is the most crucial factor for their good tribological properties. The common characteristics of the doped-TMD films in the present work and results in the literature referred to above lead us to believe that a similar process could take place in most TMD-based systems.

The self-healing capacity of the films was also verified in different compositions and conditions. Our results supported the hypothesis that a TMD-based coating co-sputtered with an adequate dopant material can exhibit very good tribological performance in humid air with improved load-bearing capacity and improved adhesion.

References used in the thesis statement

[1] Gwidon W. Stachowiak, and Andrew W. Batchelor, *Engineering Tribology*, 2nd Ed., Butterworth-Heinemann, 2001.

[2] Yu. N. Drozdov, N. V. Lukashina, and T. I. Nazarova. Using the achievements in tribology for teaching technical disciplines, *J. Mach. Manuf. Reliab.* 40 (2011) 97.

[3] S. Hogmark, S. Jacobson, and M. Larsson. Design and evaluation of tribological coatings, *Wear* 246 (2000) 20.

[4] A. A. Voevodin, J. P. O'Neill, and J. S. Zabinski. Nanocomposite tribological coatings for aerospace applications, *Surf. Coat. Technol.* 116-119 (1999) 36.

[5] A. R. Lansdown, *Molybdenum Disulfide Lubrication*, Elsevier, 1999.

[6] C. Donnet, and A. Erdemir. Solid lubricant coatings: recent developments and future trends, *Tribol. Lett.* 17 (2004) 389.

[7] A. A. Voevodin, and J. S. Zabinski. Supertough wear-resistant coatings with 'chameleon' surface adaptation, *Thin Solid Films* 370 (2000) 223.

[8] K. J. Wahl, L. E. Seitzmann, R. N. Bolster, and I. L. Singer. Low-friction, high-endurance, ion-beam-deposited Pb-Mo-S coatings, *Surf. Coat. Technol.* 73 (1995) 152.

[9] T. Polcar, and A. Cavaleiro. Self-adaptive low friction coatings based on transition metal dichalcogenides, *Thin Solid Films* 519 (2011) 4037.

[10] Ali Erdemir, Julien Fontaine, and Cristophe Donnet, "An Overview of Superlubricity in Diamond-like Carbon Films", in: Christophe Donnet, Ali Erdemir (Eds.), Tribology of diamond-like carbon films: fundamentals and applications, Springer, 2008.

[11] P. D. Fleischauer. Fundamental aspects of the electronic structure, materials properties and lubrication performance of sputtered MoS2 films, *Thin Solid Films* 154 (1987) 309.

[12] E. Benavente, M.A. Santa Ana, F. Mendizábal, and G. González. Intercalation chemistry of molybdenum disulfide, *Coord. Chem. Rev.* 224 (2002) 87.

[13] S. V. Prasad, N. T. McDevitt, and J. S. Zabinski. Tribology of tungsten disulfide films in humid environments: The role of a tailored metal-matrix composite structure, *Wear* 230 (1999) 24.

[14] Lucile Joly-Pottuz, and Fabrice Dassenoy, "Nanoparticles made of metal dichalcogenides", in: Jean M. Martin, Nobue Ohmae (Eds.), *Nanolubricants*, Wiley-Blackwell, 2008.

[15] A. Nossa, and A. Cavaleiro. Chemical and physical characterization of C(N)-doped W–S sputtered films, *J. Mater. Res.* 19 (2004) 2356.

[16] A. Nossa, A. Cavaleiro, N. J. M. Carvalho, B. J. Kooi, and J. Th. M. De Hosson. On the microstructure of tungsten disulfide films alloyed with carbon and nitrogen, *Thin Solid Films* 484 (2005) 389.

[17] A. Nossa, and A. Cavaleiro. The influence of the addition of C and N on the wear behaviour of W-S-C/N coatings, *Surf. Coat. Technol.* 142-144 (2001) 984.

[18] T. Polcar, M. Evaristo, and A. Cavaleiro. Friction of Self-Lubricating W-S-C Sputtered Coatings Sliding Under Increasing Load, *Plasma Process. Polym.* 4 (2007) S541.

[19] T. Polcar, M. Evaristo, and A. Cavaleiro. Self-Lubricating W–S–C Nanocomposite Coatings, *Plasma Process. Polym.* 6 (2009) 417.

[20] Andrey A. Voevodin, "Hard DLC Growth and Inclusion in Nanostructured Wear-protective Coatings", in: Christophe Donnet, Ali Erdemir (Eds.), *Tribology of diamond-like carbon films: fundamentals*

and applications, Springer, 2008.

[21] T. Polcar, M. Evaristo, and A. Cavaleiro. Comparative study of the tribological behavior of self-lubricating W–S–C and Mo–Se–C sputtered coatings, *Wear* 266 (2009) 388

[22] Hans-Jürgen Butt, Karlheinz Graf, and Michael Kappl, *Physics and Chemistry of Interfaces*, Wiley-VCH, 2003.

[23] David Brandon, and Wayne D. Kaplan, *Microstructural Characterization of Materials*, 2nd Ed., John Wiley & Sons, 2008.

[24] S. Ramalingam, and L. Zheng. Film-substrate interface stresses and their role in the tribological performance of surface coatings, *Tribol. Int.* 28 (1995) 145.

[25] John R. Ferraro, Kazuo Nakamoto, and Chris W. Brown, *Introductory Raman Spectroscopy*, 2nd Ed, Elsevier, 2003.

[26] Joseph B. Slater, James M. Tedesco, Ronald C. Fairchild, and Ian R. Lewis, "Raman Spectroscopy and the Industrial Environment", in: Ian R. Lewis, H. Edwards (Eds.), *Handbook of Raman Spectroscopy: from the research laboratory to the process line*, CRC Press, 2001.

[27] Mario Birkholz, *Thin Film Analysis by X-Ray Scattering*, Wiley-VCH, 2006.

[28] T. Polcar, F. Gustavsson, T. Thersleff, S. Jacobson, and A. Cavaleiro. Complex frictional analysis of self-lubricant W-S-C/Cr coating, *Faraday Discuss.* 156 (2012) 383.

[29] M. Evaristo, A. Nossa, and A. Cavaleiro. W–S–C sputtered films: Influence of the carbon alloying method on the mechanical properties, *Surf. Coat. Technol.* 200 (2005) 1076.

[30] B. C. Windom, W. G. Sawyer, and D. W. Hahn. A Raman Spectroscopic Study of MoS2 and MoO3: Applications to Tribological Systems, *Tribol. Lett.* 42 (2011) 301.

[31] A. C. Ferrari, "Non-destructive Characterisation of Carbon Films", in: Christophe Donnet, Ali Erdemir (Eds.), *Tribology of diamond-like carbon films: fundamentals and applications*, Springer, 2008.

[32] M. Regula, C. Ballif, J. Moser, and F. Lévy. Structural, chemical, and electrical characterisation of reactively sputtered WSx thin films, *Thin Solid Films* 280 (1996) 67.

[33] J.-P. Hirvonen, J. Koskinen, J. R. Jervis, and M. Nastasi. Present progress in the development of low friction coatings, *Surf. Coat. Technol.* 80 (1996) 139.

[34] National Institute of Standards and Technology, NIST X-ray Photoelectron Spectroscopy Database, 2000. (URL: **http://srdata.nist.gov/xps/**)

[35] P. M. Sousa, A. J. Silvestre, N. Popovici, and O. Conde. Morphological and structural characterization of CrO2/Cr2O3 films grown by Laser-CVD, *Appl. Surf. Sci.* 247 (2005) 423.

[36] A. A. Voevodin, J. Bultman, and J. S. Zabinski. Investigation into three-dimensional laser processing of tribological coatings, *Surf. Coat. Technol.* 107 (1998) 12.

[37] C. D. Wagner, W. H. Riggs, C. E. David, J. F. Moulder, and G. E. Muilenberg in: *Handbook of X-ray photoelectron spectroscopy*, Perkin-Elmer Corporation, 1979.

[38] P. D. Fleischauer, and J. R. Lince. A comparison of oxidation and oxygen substitution in MoS2 solid film lubricants, *Tribo. Int.* 32 (1999) 627.

[39] V. Rigato, G. Maggioni, A. Patelli, D. Boscarino, N. M. Renevier, and D.G. Teer. Properties of sputter-deposited MoS2/metal composite coatings deposited by closed field unbalanced magnetron sputter ion plating, *Surf. Coat. Technol.* 131 (2000) 206.

[40] T. Kubart, T. Polcar, L. Kopecký, R. Novák, and D. Nováková. Temperature dependence of tribological properties of MoS2 and MoSe2 coatings, *Surf. Coat. Technol.* 193 (2005) 230.

List of candidate's work relating to the doctoral thesis

Peer-reviewed articles in impacted journals

[41] J. V. Pimentel, T. Polcar, and A. Cavaleiro. Structural, mechanical and tribological properties of Mo-S-C solid lubricant coating, *Surface and Coatings Technology* vol. 205 (2011), pages 3274–3279. (Contribution: 45%)

[42] J. V. Pimentel, T. Polcar, M Evaristo, and A. Cavaleiro. Examination of the tribolayer formation of a self-lubricant W–S–C sputtered coating, *Tribology International* vol. 47 (2012), pages 188–193. (Contribution: 50%)

Other publications

[43] J. V. Pimentel, M. Evaristo, A. Cavaleiro, and T. Polcar, "Tribological Behavior of Self-Lubricating Mo-S-C Coatings", *Twelfth International Conference on Plasma Surface Engineering (PSE 2010)*, Garmisch-Partenkirchen, Germany, Sep. 13-17, 2010.

[44] J. V. Pimentel, M. Evaristo, T. Polcar, and A. Cavaleiro, "Scratch Resistance of Self-Lubricating Thin Films Based on TMDs Alloyed with Carbon", *11th European Vacuum Conference (EVC-11)*, Salamanca, Spain, Sep. 20-24, 2010.

[45] M. Evaristo, J. V. Pimentel, T. Polcar, and A. Cavaleiro, "Characterization of TMD-C doped with Ti deposited by PVD Magnetron Sputtering", *11th European Vacuum Conference (EVC-11)*, Salamanca, Spain, Sep. 20-24, 2010.

[46] T. Vitu, J. V. Pimentel, P. Siroky, M. Evaristo, A. Cavaleiro, and T. Polcar, "W-doped carbon coatings - determination of friction and wear mechanisms", *8th Asian-European International Conference on Plasma Surface Engineering (AEPSE 2011)*, Dalian, China, Sep. 19-22, 2011.

[47] J. V. Pimentel, M. Evaristo, T. Polcar, and A. Cavaleiro, "Tungsten Disulphide Films Alloyed With Chromium Deposited by D.C. Magnetron Sputtering", *International Tribology Conference Hiroshima 2011 (ITC 2011)*, Hiroshima, Japan, Oct. 03 - Nov. 04, 2011.

[48] J. V. Pimentel, F. Gustavsson, T. Polcar, and A. Cavaleiro, "Effect of surface defects on the tribology of WSC-Cr self-lubricant coatings", *European Materials Research Society Spring Meeting (E-MRS 2012)*, Strasbourg, France, May 14-18, 2012.

[49] J. V. Pimentel, M. Evaristo, T. Polcar, and A. Cavaleiro, " Self-lubricating W-S-C-Cr tribological coatings deposited by r.f. magnetron sputtering", *Thirteenth International Conference on Plasma Surface Engineering (PSE 2012)*, Garmisch-Partenkirchen, Germany, Sep. 10-14, 2012.

[50] J. V. Pimentel, M. Danek, T. Polcar, and A. Cavaleiro. Effect of patterned surface on the tribology of W-S-C/Cr self-lubricant coatings. Submitted to *Surface and Coatings Technology*, 2013.

Citations of [41]

[51] T. Polcar, and A. Cavaleiro. Review on self-lubricant transition metal dichalcogenide nanocomposite coatings alloyed with carbon, *Surf. Coat. Technol.* 206 (2011) 686.

[52] A. Shtertser, C. Muders, S. Veselov, S. Zlobin, V. Ulianitsky, X. Jiang, and V. Bataev. Computer controlled detonation spraying of WC/Co coatings containing MoS2 solid lubricant, *Surf. Coat. Technol.* 206 (2012) 4763.

Citations of [42]

[53] X.-F- Yang, P.-L. Song, S.-R. Wang, L.-Y. Yang, and Y.-J. Wang. Wear properties of self-lubricating Al2O3/TiC/CaF2 ceramic composites, *Rengong Jingti Xuebao* 41 (2012) 1741.

List of candidate's work unrelated to the doctoral thesis

[54] G. S. Beserra, J. F. Eusse, A. M. Sampaio, J. V. Pimentel, and R. P. Jacobi, "A VHDL-AMS Co-Simulation of a System on Chip for Wireless Sensor Networks", *XVI IBERCHIP Workshop (IBERCHIP 2010)*, Foz do Iguaçu, Brazil, Feb. 23-25, 2010.

[55] J. V. Pimentel, and J. C. Costa, "A Methodology for Describing Analog/Mixed-Signal Blocks as IP", *IP-Embedded Systems Conference (IP/ESC'09)*, Grenoble, France, Dec. 01-03, 2009. Published online as full article in Design & Reuse, 2009. (URL: **http://www.design-reuse.com/articles/25000/analog-mixed-signal-ip-description.html**)

[56] J. V. Pimentel, D. C. Cafe, J. E. G. Medeiros, G. S. Beserra, L. C. Neves, J. G. Guimaraes, and J. C. Costa, "An Introductory Course in VLSI CMOS Design", *Edutech 2009*, Florianópolis, Brazil, Oct. 15-16, 2009.

[57] J. V. Pimentel, and J. C. Costa, "VHDL-AMS Modeling of Analog/Mixed-Signal IP Blocks", *9th Microelectronics Student Forum Chip on the Dunes (SForum 2009)*, Natal, Brazil, Aug. 31–Sep. 03, 2009.

Summary

Thin films composed of transition metal dichalcogenides have been used in the past as solid lubricants for their good tribological properties, especially in vacuum or dry conditions. However, pure TMD coatings typically exhibit low hardness, poor adhesion, and are susceptible to detrimental effects of humidity. Doping TMD films is an approach that has been shown to improve their mechanical properties and tribological performance.

In this thesis, self-lubricant thin films based on doped TMDs (particularly molybdenum and tungsten disulfides) are investigated. The focus is kept on their tribological performance in humid air. Numerous factors that influence the films' properties and tribological behaviour – such as deposition parameters, choice and concentration of dopant element(s), and testing conditions – are analysed and discussed. The characterisation of the coatings and the results obtained are presented in detail.

The coatings were deposited in several different chemical compositions. They were examined in their as-deposited state as well as during and after tribological tests. Their characterisation was carried out using various experimental techniques, among them new methods and innovative approaches. The coatings exhibited improvements in load-bearing capacity, adhesion, and tribological properties in comparison with pure TMD films. Common traits could be observed among the different compositions, which helped elucidate the characteristics of TMD-based films in general, including the role of the dopants on the improvement of hardness and on the formation of a low-friction tribolayer. It was possible to verify the adaptive and self-lubricating characteristics of the films and to gain a further understanding of how they originate.

Shrnutí

Povlaky dichalkogenidů přechodových kovů byly v minulosti úspěšně použity jako pevná maziva, z důvodu jejich dobrých tribologických vlastností zejména ve vakuu a v podmínkách suchého tření. Nedopované povlaky dichalkogenidů přechodových kovů ale mají nízkou tvrdost, slabou adhezi k substrátu a podléhají škodlivým vlivům vlhkosti. Dopování těchto vrstev je tudíž způsob, jak zlepšit jejich mechanické a tribologické vlastnosti.

V této disertační práci jsou studovány povlaky dichalkogenidů přechodových kovů dopované disulfidy molybdenu a wolframu. Hlavním cílem je analyzovat jejich tribologické vlastnosti ve vlhkém vzduchu a zkoumat vliv faktorů, které tribologické vlastnosti ovlivňují. Podrobně jsou diskutovány nejdůležitější faktory, kam patří parametry depozičního procesu, výběr dopujících prvků a jejich koncentrace a v neposlední řadě i volba podmínek tribologických testů.

Pro experimentální část byly připraveny povlaky s různým chemickým složením. V první části byly povlaky analyzovány ve stavu po deponování a poté během a po tribologických testech. Charakterizace vrstev byla provedena různými experimentálními technikami, z nichž některé jsou nové či inovativní. Z výsledků bylo zjištěno, že dopované povlaky dichalkogenidů přechodových kovů mají vyšší únosnost, adhezi k substrátu a tribologické vlastnosti v porovnání s nedopovanými povlaky. Při porovnání povlaků s různým chemickým složením byly pozorovány podobné rysy, čímž bylo možné objasnit charakteristické vlastnosti zkoumaných povlaků, zejména vliv dopujících prvků na zvýšení tvrdosti a vytváření třecí mezivrstvy při tření. S pomocí tohoto přístupu bylo možné ověřit jejich adaptivní a samomazné vlastnosti a zároveň pochopit podstatu mimořádných vlastností dichalkogenidů přechodových kovů.